Inversion using Euler deconvolution of the magnetic gradient tensor

Phillip W. Schmidt
CSIRO Industrial Physics
PO Box 218
Lindfield NSW 2070
Phil.Schmidt@csiro.au

SUMMARY

While the routine measurement of the magnetic gradient tensor is some way off, in certain circumstances it is possible to calculate the gradient tensor from total magnetic intensity (TMI) information. Such circumstances include anomalies being no more than about 20 percent of the local Earth's field, where the field departs from being a true potential field, and adjacent lines being well levelled.

Euler deconvolution requires solving at least four simultaneous homogeneous equations to yield the location in 3D and the Euler structural index of the source. Combining two or more adjacent tensors provides an over-determined system which allows the covariance to be estimated and gives a measure of uncertainty.

This method extracts a wealth of information on the location and geometry of magnetic sources. However, the method is sensitive to departures of the TMI from being a true potential field, for very strong anomalies, in which case conversion to a true potential can be performed using an iterative method involving calculating components from the TMI and projecting the components onto the local field direction.

Key words: magnetic, survey, inversion, tensor, Euler

INTRODUCTION

While the measurement of total magnetic intensity (TMI) gradients is now fairly common-place, the measurement of the full magnetic gradient tensor is still in its infancy (Christensen and Rajagopalan, 2000; Schmidt and Clark, 2000; Heath et al., 2003). However, it is well known that, in principle, any quantity such as components or their gradients can be calculated if the magnetic field is known with sufficient spatial resolution and precision everywhere on a grid above the source (Nelson, 1988; Blakely, 1996).

The magnetic gradient tensor offers a number of new interpretation schemes to answer specific questions about the location and shape of the source. For instance, the first invariant I_1 outlines source boundaries and appears to have superior resolving power to the analytic signal. This follows from its faster fall-off rate.

$$I_1 = B_{xx}B_{yy} + B_{yy}B_{zz} + B_{zz}B_{xx} - B_{xy}^2 - B_{yz}^2 - B_{zx}^2 \quad (1)$$

The second invariant I_2 preferentially outlines shallower features of complex sources, because of its higher fall-off rate than I_1.

$$I_2 = DET\ \left[B_{ij}\right] = B_{xx}\left(B_{yy}B_{zz} - B_{yz}^2\right) + B_{xy}\left(B_{yz}B_{xz} - B_{xy}B_{zz}\right) + B_{xz}\left(B_{xy}B_{yz} - B_{xz}B_{yy}\right) \quad (2)$$

Here another interpretation scheme, tensor Euler deconvolution, is presented that has the advantage of simultaneously mapping the location and geometry of magnetic sources.

METHOD AND RESULTS

Tensor Euler deconvolution was introduced by Zhang et al. (2000) for analysing and interpreting gravity tensor gradiometer data. Its extension to the magnetic tensor is ineluctable. Euler deconvolution as normally applied to TMI surveys makes use of the following relationship:

$$x\frac{\partial B}{\partial x} + x\frac{\partial B}{\partial y} + x\frac{\partial B}{\partial z} + = -nB \quad (3)$$

where B is the anomalous field and n is Euler's structural index (Blakely, 1996; Schmidt et al., 2004). The same relationships apply to gradients of components,

$$x\frac{\partial B_x}{\partial x} + x\frac{\partial B_x}{\partial y} + x\frac{\partial B_x}{\partial z} + = -nB_x \quad (4)$$

and by extension, to the gradient tensor. Allowing for an arbitrary origin the following matrix equation is arrived at,

$$\begin{bmatrix} \frac{\partial B_x}{\partial x} & \frac{\partial B_x}{\partial y} & \frac{\partial B_x}{\partial z} \\ \frac{\partial B_y}{\partial x} & \frac{\partial B_y}{\partial y} & \frac{\partial B_y}{\partial z} \\ \frac{\partial B_z}{\partial x} & \frac{\partial B_z}{\partial y} & \frac{\partial B_z}{\partial z} \end{bmatrix} \begin{bmatrix} x - x_0 \\ y - y_0 \\ z - z_0 \end{bmatrix} = -n \begin{bmatrix} B_x \\ B_y \\ B_z \end{bmatrix} \quad (5)$$

Since there are four unknowns, n, x, y and z, at least two tensors are required for each source to solve (5) in a least-squares fashion. Two adjacent tensor form a 6 × 3 matrix and successive tensors are added to the top and the bottom 3 × 3. In practice, as many tensors are combined as possible until the

variance exceeds some predetermined cut-off. The variance is calculated using the method of Hext (1963).

Examples

To test the above concepts two models were used. These were a spherical and a prism source. The anomalous magnetic components and their gradients, which comprise the gradient tensor, were calculated on a regular grid 100 m above for both sources. The sphere had a radius of 50 m, and the prism, which is vertically extended, had a square cross-section with sides of 50 m. These sources have structural Euler indices of 3 and 2 respectively. Note that at low heights, say 10 m, compared to the length of the sides (50 m), the index for the prism would be complicated, approaching that of a vertical contact near the centre of the sides (n ~ 0.5). However, at heights greater than twice the length of the sides the index for the prism approaches that of a vertical cylinder, for which n = 2.

The components were calculated using the algorithms of Emerson et al. (1985). Whereas the gradients comprising the tensors for the sphere were calculated by differentiating the terms for the components, the gradients for the prism were calculated using Fourier filtering (Nelson, 1988).

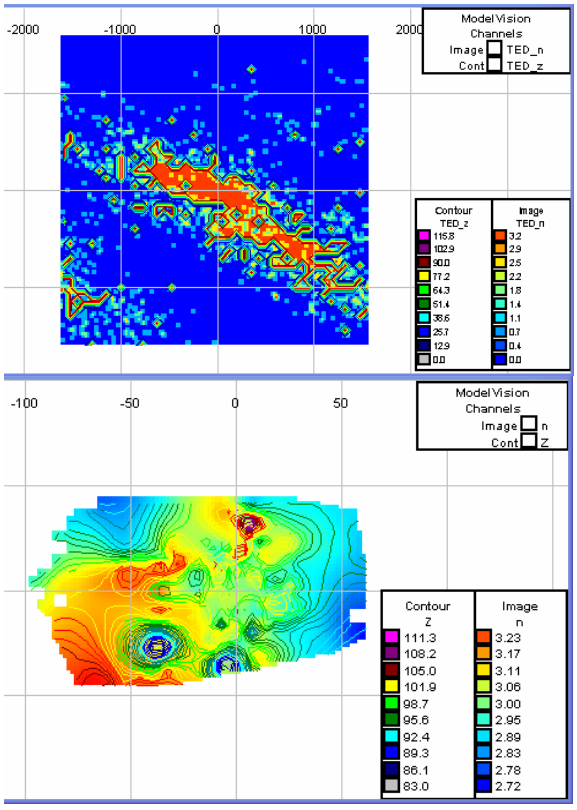

Figure 1. Results for the spherical source showing locations where solution were found for the source (top) versus the actual solutions using Euler deconvolution of the gradient tensor calculated on the same grid (bottom). Solutions were found spread along a NW-SE trend localising the source to a few tens of metres. The solutions are consistent with an Euler structural index for a spherical source (n = 3) at 100 m depth.

The locations in the survey area where acceptable solutions were found and the results from tensor Euler deconvolution for both types of sources are shown in Figures 1 and 2. The upper image of each figure shows the survey locations where the solutions were found, colour coded according to the Euler structural index and contoured according to depth. The actual solutions are given in the lower image of the figures localising the source at, or close to, the origin. No solutions with a variance below the chosen cut-off were found that indicated the source was outside the areas shown in the lower images of the figures. Note that the grid for the solutions (a few 10s of metres square) is much smaller than the grid for the whole survey which was 3.2 km × 3.2 km. In the figures Euler's structural index is plotted as an RGB image, while the depth is plotted as contours. At this point it is unknown why acceptable solutions are found at observation points spread from NW to SE of the sources, however, this seems to be the case for both the sphere and the pipe.

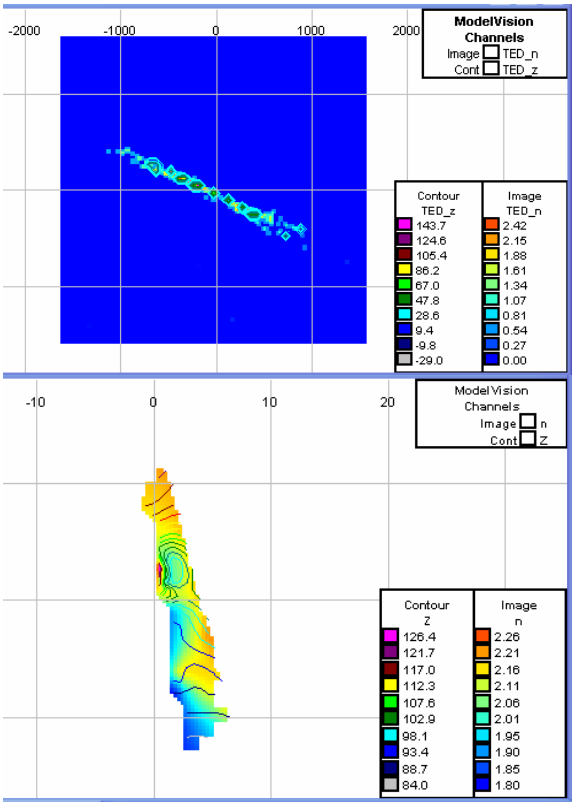

Figure 2. Results for the prism (pipe-like) source showing locations where solution were found for the source (top) versus the actual solutions using Euler deconvolution of the gradient tensor calculated on the same grid (bottom). As for the spherical source, solutions were found spread along a NW-SE trend localising the source to a few tens of metres. The solutions are consistent with an Euler structural index for a pipe-like source (n = 2) at 100 m depth.

The acceptable solutions for the spherical source (bottom of Figure 1) fix the centre of the body within a few tens of metres of its modelled position. The most reliable solutions locate the centre precisely at 0 m north, 0 m east and 100 m below.

The acceptable solutions for the pipe-like source (bottom of Figure 2) also fix the centre of the body within a few tens of

metres of its position, although solutions are spread in a thin NS linear trend up to 20 m south of the epicentre. Given the sides of the pipe are 50 m wide this is not a great error.

For both the sphere and the pipe source, drilling vertically anywhere within the most reliable solution zone would intersect the source body.

CONCLUSIONS

Tensor Euler deconvolution is a useful tool to extract and visualise more information from the magnetic field. In the future, when airborne tensor measurements will become routine, tensor Euler deconvolution will be the first step in data analysis. At the present time though, tensor Euler deconvolution may be applied to a TMI survey if the survey is of sufficient quality.

ACKNOWLEDGEMENTS

I would like to thanks my colleagues Keith Leslie, Marcel Bick and Cathy Foley for critically commenting on drafts of this article and for their encouragement.

REFERENCES

Blakely, R.J., 1996, Potential theory in gravity and magnetic applications: *Cambridge University Press*, Cambridge, pp. 441.

Christensen, A. and Rajagopalan, Shanti, 2000, The magnetic vector and gradient tensor in mineral and oil exploration: Preview, 84, 77.

Emerson, D.W., Clark, D.A. and Saul, S.J., 1985, Magnetic exploration models incorporating remanence, demagnetisation and anisotropy: HP 41C handheld computer algorithms: Exploration Geophysics, 16, 1-122.

Heath, P., Heinson, G. and Greenhalgh, S., 2003, Some comments on potential field tensor data: Exploration Geophysics, 34, 57-62.

Hext, George R., 1963. The estimation of second-order tensors, with related tests and designs: Biometrika, 50, 353-373.

Nelson, J.B., 1988, Calculation of the magnetic gradient tensor from total field gradient measurements and its application to geophysical interpretation: Geophysics, 53, 957-966.

Schmidt, P.W. and Clark, D.A., 2000, Advantages of measuring the magnetic gradient tensor: Preview, 85, 26-30.

Schmidt, P., Clark, D., Leslie, K., Bick, M., Tilbrook, D. and Foley, C., 2004. GETMAG – A SQUID magnetic tensor gradiometer for mineral and oil exploration: Exploration Geophysics, 35, 297-305.

Zhang, Changyou, Mushayandevu, M.F., Reid, A.B., Fairhead, J.D. and Odegard, M.E., 2000, Euler deconvolution of gravity tensor gradient data: Geophysics, 65, 512-520.